Evaluation of a charcoal from cistus Ladaniferus seeds used as an adsorbent for anionic dye removal from aqueous phases

H. El Farissi[1], R. Lakhmiri[1*], A. Albourine[2], M. Safi[3] and Omar Cherkaoui[4]

Abstract— Environmental pollution by either solid or liquid pollutants is a big problem in our ecosystem. The environmental cleanup can be carried out according to several types of processes by; solid waste discharge, coagulation flocculation, chemical precipitation, decantation, floating, filtration, etc. But all these techniques are used to transfer pollution from one environment to another. The increasing demand for adsorbents used in environmental protection processes has made their price more and more expensive, leading to further research into the production of new, cheaper adsorbent materials from non-conventional materials, concretely from biomass. The valorization of the charcoal of seeds from cistus Ladaniferus, produced by pyrolysis as a bioadsorbant of anionic dyes, the red reactive 23 (RR-23) was carried out. The influence study of the various parameters such as temperature, pH, adsorbent dose, initial concentration and contact time were carried out. The kinetics adsorption of dye by BC-CLS, CAa-CLS and Cab-CLS are correctly described by the pseudo-second order model with a correlation factor (R^2 = 0.997), (R^2=0.996) and (R^2 = 0.995) respectively. As for the modeling of the adsorption isotherm, among the four models tested, Langmuir model is most appropriate with a correlation factor equal to (R^2=0.9948), (R^2 = 0.9969 and (R^2 = 0.9966) for the BC-CLS, CAa-CLS and the Cab-CLS respectively. On the other hand, the ability to remove the dye by the BC-CLS is advantageous and the elimination efficiency reaches a maximum value of 99.237% for the CAa-CLS and 92% for the CAb-CLS.

Index Terms— Charcoal - Isotherm - Adsorption - Cistus Seeds – dye - Reactive red 23 - waste water - Technical analysis .

Graphical Abstract

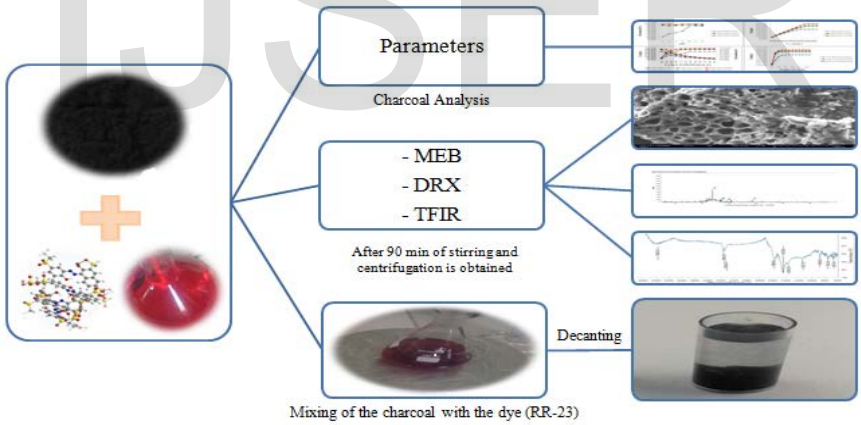

1. INTRODUCTION

Morocco has a large forest area which ensures a large annual production of biomass for different purposes (timber, firewood, fire charcoal production, pulp production etc ...), but the seeds and shells of some wild biomass follow no valorization except some production of essential oils. Fixed-bed pyrolysis of cistus Ladaniferus seeds produced the biochar [1].

- *H. El Farissi, Laboratory of Chemical Engineering and Valorization of the Resources, Faculty of Sciences and Techniques of Tangier, AbdelmalekEssaâdi University, Km 10 route de Ziaten, BP 416 Tangier, Morocco.*
- *R. Lakhmiri, Laboratory of Chemical Engineering and Valorization of the Resources, Faculty of Sciences and Techniques of Tangier, AbdelmalekEssaâdi University, Km 10 route de Ziaten, BP 416 Tangier, Morocco. PH:+212661427257 lakhmirir@yahoo.fr*
- *A. Albourine, Laboratory of Materials and Environment, Team of Coordination Chemistry, Faculty of Sciences, IbnZohr University, BP 8106, 80000 Agadir, Morocco.*
- M. Safi, *Laboratory of Physical Chemistry and Bio-Organic Chemistry, URAC University of Hassan II Mohammedia- Casablanca, Faculty of Sciences and Techniques-Mohammedia, BP 146,Mohammedia, Morocco*
- *O. Cherkaoui, Laboratory REMTEX, Higher School of Textile and Clothing Industries, Casablanca, Morocco*

The growth of the textile industry is expected to produce several effluents in the factories, the latter are rich in dyes that pose several problems. The elimination of these dyes by the adsorption method is the most used. Several studies have been done on the elimination of dyes by activated charcoal of different biomass but the activated charcoal of cistus seeds was never made, so the valorization of bioressource such as biochar of seeds and shells in the removal of red reactive dye 23 (RR-23) [2], [3], presents very encouraging results, the activated biochar due to increased number of active sites and the increase of the adsorption surface by creation of new pores, so study that are made on the elimination of red reactive dye 23 on chitosan extracted from shrimp waste [4], [5]. The elimination study of methylene blue on Fish Coal (FBC) isothermal follows the Langmuir and Freundlich model and the kinetics the pseudo-second order model, the maximum amount of adsorption of BM by NaOH- BCF was 605.82mg.g^{-1} [6]. The same studies that are done in the removal of cadmium and methylene blue from wastewater by charcoal (BC), activated charcoal (BCA) and BCA/TiO2 mixture (BCA-D), the maximum adsorbed amount varies from 100mg.g^{-1}, 200mg.g^{-1} and 250mg.g^{-1} respectively [7].

2. MATERIAL AND METHODS

2.1. Preparation of activated carbon

In general, charcoal is a porous carbonaceous material. It can be prepared from several types of raw materials such as oil shale, wood, coconut shell, almond hull, olive pomace and olive kernels, etc. In this study, a charcoal is prepared from the cistus Ladaniferus by a thermal route called pyrolysis under optimal conditions the temperature equals reaches 450 °C for, the speed heating is 21 °C.min^{-1}, and the sizes of particles for seeds between 0.3 to 0.6 mm. Then we are interested in the chemical activation of our biochar[1].

2.1. Carbon Activation

2.1.1. Activation with phosphoric acid H_3PO_4

Among the acids, phosphoric acid has been widely used for the activation of charcoal [8–10]. The acid activation is carried out using phosphoric acid (H_3PO_4) with some minor modifications. BC-CLS is impregnated with a solution of H_3PO_4 at a purity percentage ≥ 85% with a weight ratio of 1:1. The mixture is heated in an oven at 100 °C for 24 hours. The char of seeds acid-activated (CAa-CLS) are washed with distilled water and then with $NaHCO_3$ solution (2M) to neutralize the acidity. Before drying at 100 °C, the CAa-CLS is washed again with distilled water, until a pH = 6 are reached in the residual water. The obtained samples are noted: Charcoal of the Cistus Ladaniferus seeds (BC-CLS), and Charcoal of the cistus Ladaniferus acid-activated seeds (CAa-CLS)

2.1.2. Activation with sodium hydroxide (NaOH)

Sodium hydroxide has also been cited in literature for the activation of coals[11, 12], 10 g of the BC-CLS is first soaked in the 97% sulfuric acid (H_2SO_4) solution (desiccant, oxidizer and mineral-removing agent) for 24 hours and then washed with distilled water until to reach a pH = 6 in the residual liquid. BC-CLS is then immersed in 200 ml of NaOH (4M) with stirring at 85 °C for 2 h. The liquid is then filtered off and the seed powder thus activated by the base (CAb-CLS) is dried at 120 °C for 24 hours. The obtained samples are noted: charcoal of the seeds of cistus Ladaniferus (BC-CLS) and charcoal of the seeds of cistus Ladaniferus activated (CAb-CLS)

2.2. Characterization of BC-CLS, CAa-CLS and CAb-CLS.

The characterization of the BC-CLS, CAa-CLS and CAb-CLS obtained were characterized by different analysis techniques. X-Ray Diffraction, SEM with Scanning Electron Microscope and Fourier Transform Infrared Spectroscopy (FTIR).

Figure 1 and 2 shows the X-ray diffractograms of CAa-CLS and CAb-CLS activated carbons. Acid activated charcoal Figure 1 and 2 (a) (CAa-CLS) have characteristic peaks at 2θ=10.48°; 21.08°; 30.08° by diffraction of the (002) and (013) planes and the planes (105) of the monoclinic P21 (4) crystalline lattices of ascorbic acid ($C_6H_8O_6$), characteristic peaks at 2θ=13 °; 15°; 25° and 28.5° representing the crystal structure of 2-butanone semicarbazone ($C_5H_{11}N_3O$) and characteristic peaks at 2θ=16.4°; 18.9°; 26.9° by diffraction of the planes (011) and (200) and the planes (220) of the cubic crystalline lattice of piperadinium nitrate ($C_5H_{12}N_2O_3$).

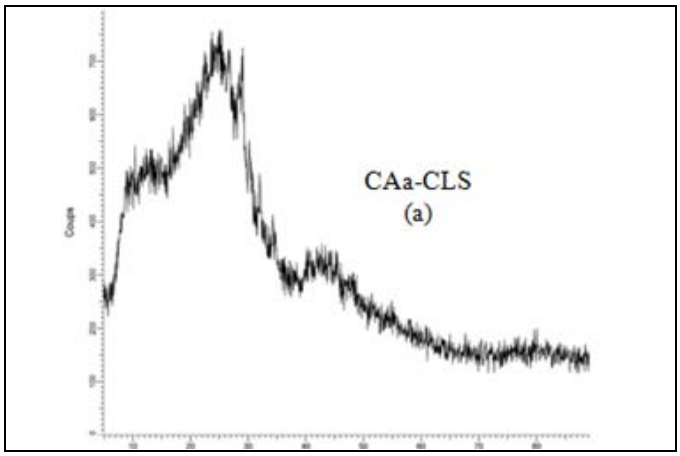

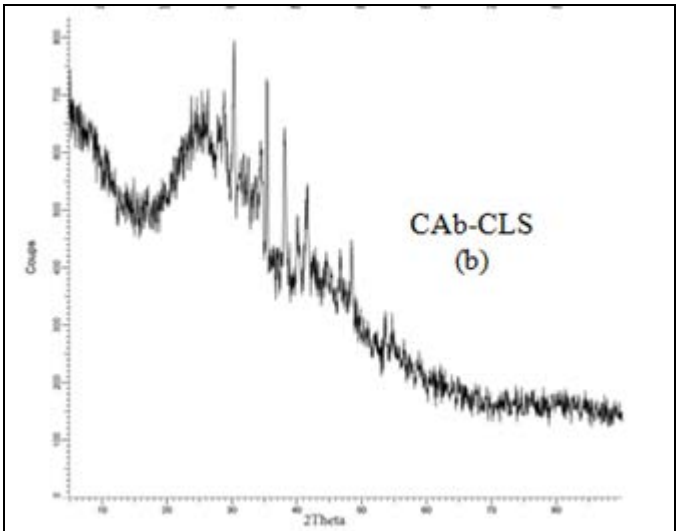

Figure .1. X-ray diffractograms of the CAa-CLS (a), CAb-CLS (b)

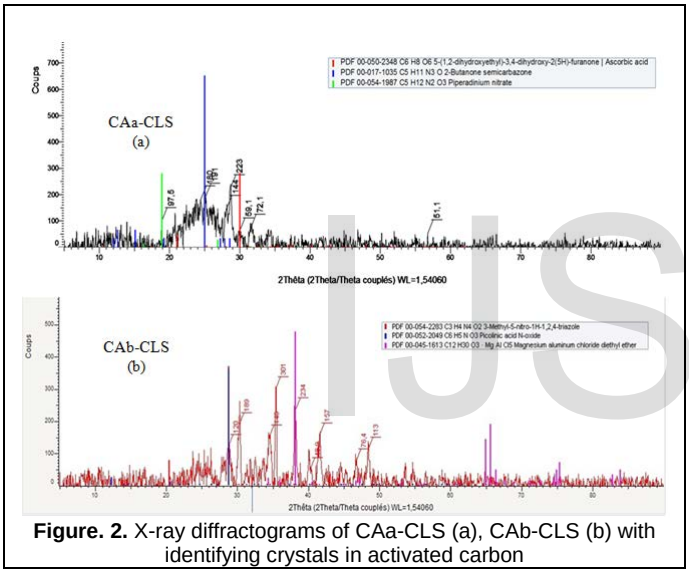

Figure. 2. X-ray diffractograms of CAa-CLS (a), CAb-CLS (b) with identifying crystals in activated carbon

The X-ray diffractograms of the basic activated carbon CAb-CLS (Figure 1 and 2, (b)) shows characteristic peaks at 2θ = 21°; 35.2°; 41.2°; 46.3° and 48.5° correspond to the crystalline structure of 3-methyl-5-nitro-1H-1,2,4-triazole ($C_3H_4N_4O_2$), which gives our charcoal very important properties such as chemical stability, characteristic peaks in 2θ = 12°; 28.8°, 54.7° and 65° by diffraction from the (001), (012), (-401) and (232) planes of the P21/m (11) monoclinic crystal lattice of picolinic acid N-oxide ($C_6H_5NO_3$) and finally characteristic peaks at 2θ=28.9°; 38.2°; 66°; 75.3° correspond to an organometallic of a crystal lattice of magnesium aluminum chloride diethyl ether ($C_{12}H_{30}O_3MgAlCl_5$). But most of the activated carbon structure is either a base or an acid is amorphous.

The SEM analysis gives a clear idea of the morphology of our materials and the number of pores increases with activation (Figure 3). This promotes the adsorption of RR-23 on the three materials.

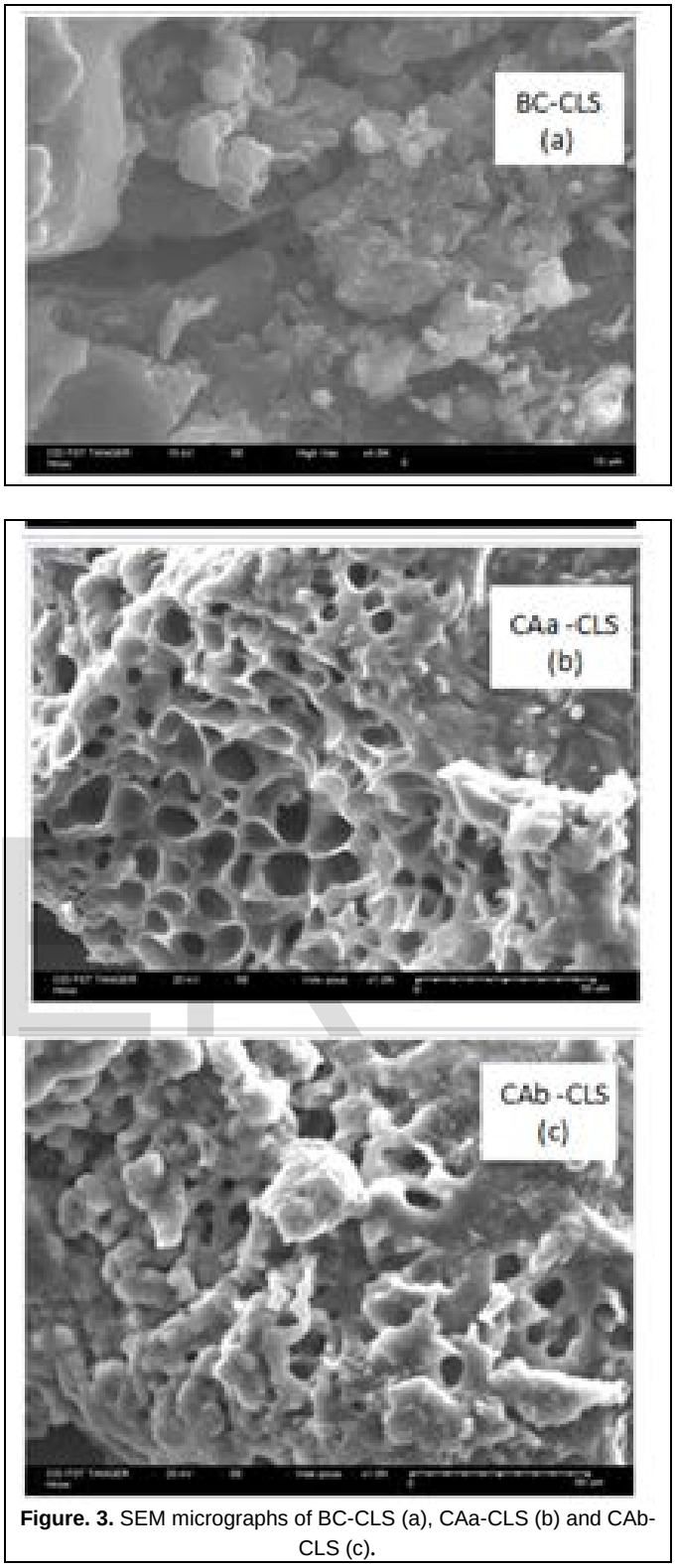

Figure. 3. SEM micrographs of BC-CLS (a), CAa-CLS (b) and CAb-CLS (c).

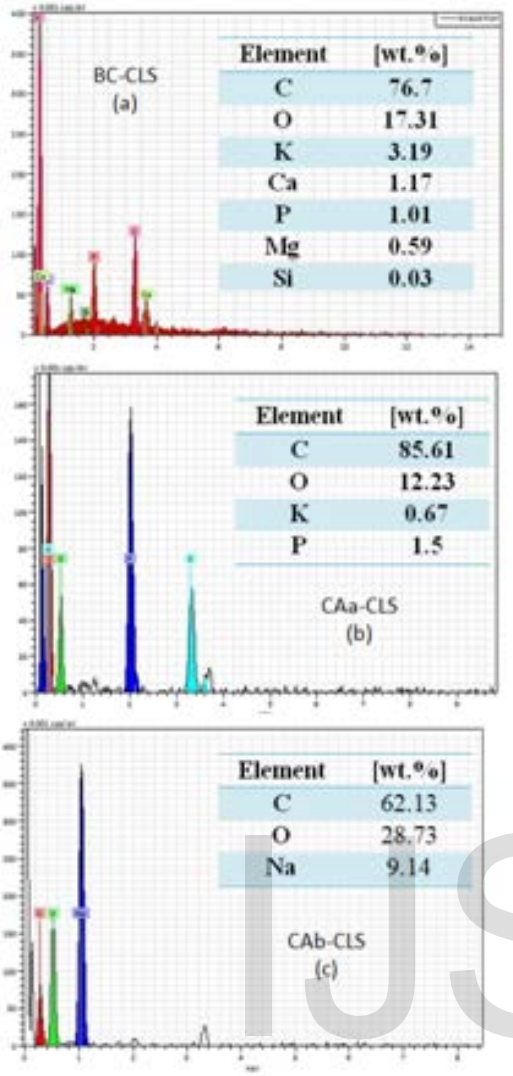

Figure .4. EDXA diffractograms of the BC-CLS (a), CAa-CLS (b) and CAb-CLS (c) before adsorption.

The EDXA spectrum of BC-CLS (a), CAa-CLS (b) and CAb-CLS (c) (Figure 4) also confirms the presence of a high percentage of carbon and oxygen in the three materials, in addition to the presence of other elements such as K, P, Mg, Ca and Si in BC-CLS.

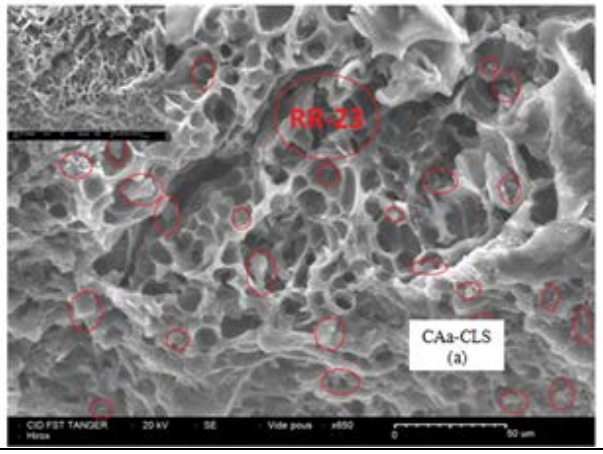

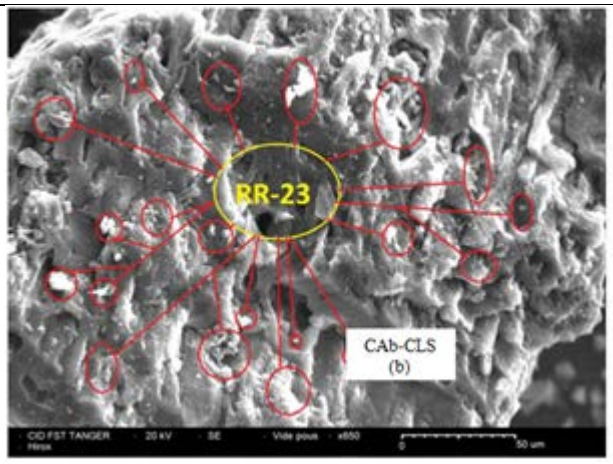

Figure .5. SEM micrographs of BC-CLS (a), CAa-CLS (b) and CAb-CLS (c) after adsorption.

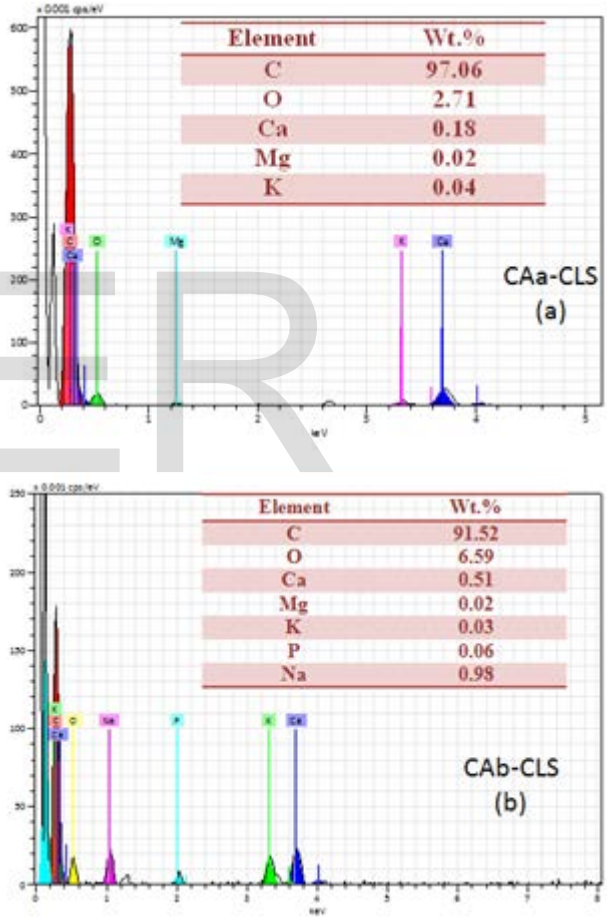

Figure .6. EDXA diffractograms of the BC-CLS (a), CAa-CLS (b) and CAb-CLS (c) after adsorption.

The figure 6 shows the EDXA spectrum of RR-23 dye adsorption on CAa-CLS (a) and CAb-CLS (b) after adsorption. The spectrum has fairly high percentages of carbon and oxygen. This is due to the fixation of the dye inside the pores and the surface of the activated carbon. Just as the SEM image also shows that the morphology of our active charcoal is modified after the adsorption and the presence of the dye in charcoal presented by the circles red in figure 5.

Infrared spectroscopy analysis of CAa-CLS and CAb-CLS, (figure7) show the OH- bonds associating phenol and alcohol functions between 3200 to 3400cm^{-1}, the C-H of cycloalkane bonds between 2850 to 2925 cm^{-1}, the phosphines between 2280 to 2410cm^{-1}, N-H of the primary amines between 1550 to 1650 cm^{-1}, the C = O carboxylic acid from 1400 to 1450 cm^{-1}, C-N of aromatic amines from 1180 to 1360 cm^{-1}, C-O of primary alcohol from 1050 to 1080 cm^{-1}, the C-O of ethers between 1000 to 1090 cm^{-1}, the Ar-C between 850 to 890 cm^{-1} and finally mono substituted aromatic from 780 to 800 cm^{-1}.

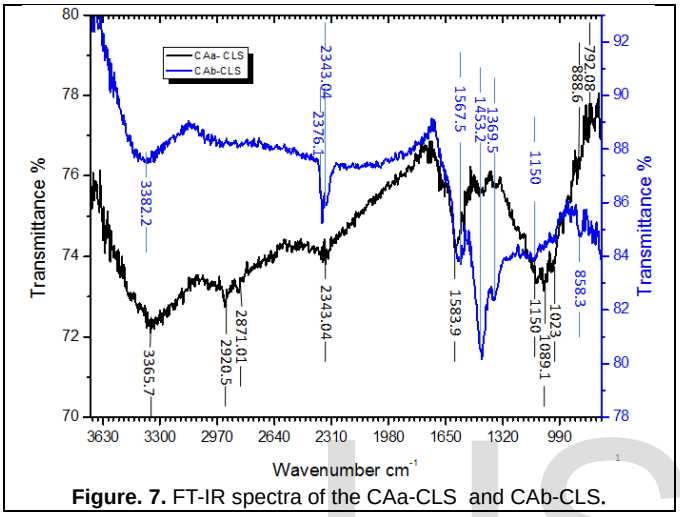

Figure. 7. FT-IR spectra of the CAa-CLS and CAb-CLS.

2.4. Adsorption Process

2.4.1. Adsorption kinetics.

The adsorption kinetics are studied only on the BC-CLS, CAa-CLS and CAb-CLS, operating under optimum conditions (PH = 10 ± 0.3, adsorbent dose [0.1- 0.2 mm] = 50 mg, dye concentration 300mg.L^{-1}, stirring speed = 200tr.min^{-1} In Erlenmeyer rode 50 mg of the adsorbent are mixed with 50 ml of the RR-23 solution (C_0=300mg.L^{-1}). The suspension is stirred at 200 rpm at room temperature (30 ±1°C). At defined time intervals ranging from 10 to 120 min, the BC-CLS, CAa-CLS and CAb-CLS are separated from the liquid by centrifugation. The concentration of the RR-23 in the liquid phase is then determined by measuring the absorbance at 511 nm and reading on a calibration curve established from a range of RR-23 concentrations ranging from 0.0 to 400mg.L^{-1}. The amount of RR-23 (Q_t) adsorbed by two materials as a function of time are calculated according to the following formula (eq.1).

$$Q_e = \frac{(C_0 - C_e)*V}{m} \quad \text{(eq.1)} \qquad R\% = \frac{(C_0 - C_e)}{C_0} * 100 \quad \text{(eq.2)}$$

C_0: concentration initial dye in (mg.L^{-1}); C_e: final dye concentration in solution (mg.L^{-1}); V: volume of the dye solution in L; m: mass of –CLS or CAa-CLS or CAb-CLS in g; R%: Removal; Q_e: Amount adsorbed in (mg.g^{-1})

The four linear models tested for adsorption kinetics of RR-23 dye by BC-CLS, CAa-CLS and CAb-CLS are shown in table 1.

TABLE 1. THE FOUR LINEAR MODELS OF KINETICS

Models	Plotting	Linear Equation
Pseudo-1st-order	$Ln(Q_e-Q_t) = f(t)$	$Ln(Q_e - Q_t) = -K_1 t + Ln\, Q_e$ [13], [14]
Pseudo-2nd-order	$= f(t)\frac{t}{Q_t}$	[15], [16] $\frac{t}{Q_t} = \frac{t}{Q_e} + \frac{1}{K_2 Q_e^2}$
Elovich	$Q_t = f(Ln(t))$	[17] $Q_e = \frac{1}{\beta} Ln\, t + \frac{1}{\beta} Ln\,(\alpha\beta)$
Intraparticule diffusion	$Q_t = f(\sqrt{t})$	[18] $Q_e = K_i \sqrt{t} + C$

Where q_e: the dye amount adsorbed at equilibrium (mg.g^{-1}), q_t: the dye amount adsorbed at time t (mg.g^{-1}), K_1 is the adsorption rate constant (mL.min^{-1}), t: contact time (min), K_2 (g.mg^{-1}.min), α is the initial adsorption capacity (mg.g^{-1}.min), β is the desorption constant (g.mg^{-1}), K_i is the intraparticule diffusion rate constant. The value of the ordinate at the origin C provides an indication of the thickness of the boundary layer.

2.4.2. Obtaining and modeling of the adsorption isotherm.

To obtain the adsorption isotherm, a series of Erlenmeyer is used. In each Erlenmeyer are poured 50 ml of RR-23 solution dye of varying concentrations: 0; 50; 100; 150; 200; 250; 300; 350; 400; 450 and 500 mg.L^{-1}. The adsorption equilibrium study is carried out under the same optimum conditions indicated above. After equilibration, the particles of the adsorbent are separated by centrifugation and the clarified solution is analyzed by determination of the equilibrium concentration (C_e) of RR-23 using the same calibration curve used previously. The quantity of the adsorbed reagent at equilibrium (Q_e, in mg.g^{-1}) is calculated by equation (eq-1). The four linear models describe the adsorption isotherms tested are the Tempkin Model, Dubinin-Radushkevich Model, Freundlich Model and Langmuir Model. The latter is the most applicable for the three adsorbents. The linearization of this model is given by the following equation.

$$Q_e = \frac{Q_m K_L C_e}{1 + K_L C_e} \quad \text{(eq.3)}$$

This equation can be reshaped and rearranged into linear of the following equations [19].

$$\frac{C_e}{Q_e} = \frac{C_e}{Q_m} + \frac{1}{Q_m K_L} \text{(eq.4)}$$

Q_e is the amount (mg.g^{-1}) of RR-23 adsorbed at equilibrium; this is the equilibrium concentration (mg.L^{-1}); Q_0: the monolayer adsorption capacity (mg.g^{-1}); K_L: the Langmuir constant (L.mg^{-1}) related to the adsorption free energy.

An essential characteristic of the Langmuir isotherm can be expressed in terms of a dimensionless constant called the separation factor and defined by the equation below [20].

$$R_L = \frac{1}{1 + K_L C_0} \quad \text{(eq.5)}$$

Where C_0 is the initial concentration of the adsorbate (mg.L^{-1}) and K_L is the Langmuir constant (L.mg^{-1}). A

separation factor $R_L > 1$ indicates that the adsorption is unfavorable, if $R_L = 1$ the adsorption is said to be linear, adsorption is said to be favorable when $0 < R_L < 1$, and a zero separation factor ($R_L = 0$) Indicates that adsorption is irreversible. In our case, the found values of R_L are all between 0 and 1, which reveals favorable adsorption.

3. RESULTS AND DISCUSSION

3.1. Study of the elimination of RR-23 dye by BC-CLS, CAa-CLS and CAb-CLS.

The study of the adsorption kinetics is carried out on the pyrolyzed and activated carbon of cistus Ladaniferus seeds, operating under optimal conditions (pH = 10 ± 0.3, the mass = 50 mg, the concentration C_0 = 300 $mg.L^{-1}$, the temperature T = 30 ± 1°C and stirring 200 rpm). In Erlenmyer flasks 50 mg of the adsorbent are mixed with 50 ml of the RR-23 solution (C_0=300$mg.L^{-1}$). The suspension is stirred at 200 rpm at room temperature (30 ± 1 ° C). At previously defined time intervals (in the range of 10 to 120 min), BC-CLS, CAa-CLS and CAb-CLS are separated from the liquid by centrifugation. The concentration of RR-23 in the liquid phase is then determined by measuring the absorbance at 511 nm and reading on a calibration curve established from a range of RR-23 concentrations ranging from 0.0 to 45$mg.L^{-1}$. The amount of RR-23 (Q_e) adsorbed by the BC-CLS, CAa-CLS and CAb-CLS as a function of time is calculated according to the formula equation (eq 1).

3.2. Influence of pH on the adsorption capacity of RR-23

The effect of pH on the adsorption of RR-23 on the bio-char is shown in figure 8. The nearly constant adsorption efficiency from pH = 10 ± 0.3 shows a significant effect of pH on the bio-coal in the adsorbed quantity increases with the increase of the pH same observation on the raw material of the rockrose and also for the bio-coal of the seeds. On the other hand, the quantities adsorbed by the activated carbons do not have a significant change with the increase of the pH, the adsorbed quantity varies between 271.22 to 283.2 $mg.g^{-1}$ for CAa-CLS and 293 to 294.02 $mg.g^{-1}$ for CAb-CLS.

It can be concluded that the acid protons which block the active adsorption sites are neutralized by the addition of $NaHCO_3$ in the acid activation by contrast in the basic activation in addition to HO^- ions at the surface of adsorbents.

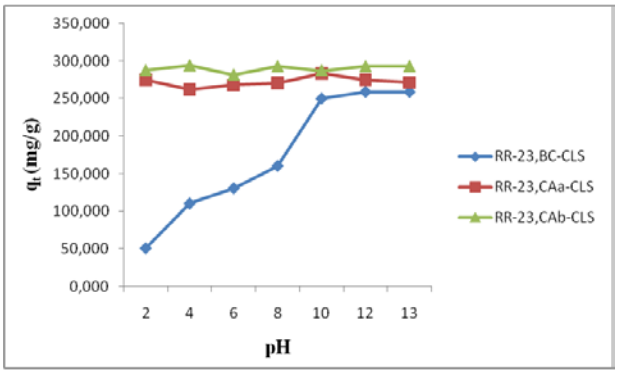

Figure .8. Effect of pH on RR-23 dye adsorption by (BC-CLS, CAa-CLS and CAb-CLS) (t = 60min, T = 30 ± 1 ° C, Adsorbent dose 50mg, Co = 300mg.L-1) stirring = 200 rpm)

3.3. The effect of the adsorbent dose on the adsorption capacity of RR-23.

The figure 9 shows that the yield of RR-23 adsorbed increases with increasing mass of BC-CLS, CAa-CLS and CAb-CLS up to an optimal value of 140 mg for BC-CLS, CAa-CLS and 100 mg for CAb-CLS. The dye removal efficiency of 80.89%, 95.85% and 99.9% respectively

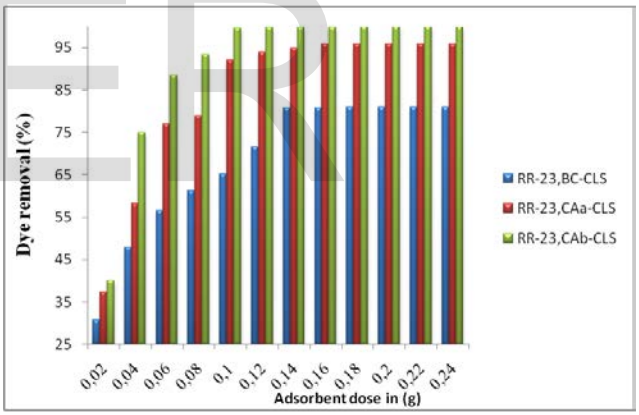

Figure 9. Effect of adsorbent quantity (BC-CL, CAa-CLS and CAb-CLS) on RR-23 dye adsorption (t = 60min, T = 30 ± 1 ° C, Co = 300mg.L-1; stirring = 200 rpm and pH = 10 ± 0.3)

3.4. The effect of the initial concentration

The effect of the initial concentration of RR-23 in the range of 50 to 600 $mg.L^{-1}$ on the removal efficiency and the amount of adsorption of RR-23. The Figure 10 shows the variation of the adsorbed quantity depending on the concentration. As the concentration increases, the elimination efficiencies of RR-23 by BC-CLS, CAa-CLS and CAb-CLS are reduced from 86.78% to 43.84% and from 93.76% to 60%. 16% and 99.29% to 70.31% respectively. The RR-23 ratio at vacant BC-CLS, CAa-CLS and CAb-CLS sites is high, resulting in increased dye removal and transfer to the absorbing surface by migration and convection at lower concentrations. 400$mg.L^{-1}$. At higher RR-23 concentrations ≥ 400 $mg.L^{-1}$, the lower clearance percentage is due to saturation of the

BC-CLS, CAa-CLS and CAb-CLS sites or a possible repulsive force between the adsorbed layers and the remaining molecules in bulk. The data show that the RR-23 uptake increases from 262.62 to 263.03 mg.g^{-1}, from 315.88 to 360.93 mg.g^{-1} and from 366.39 to 421.87 mg.g^{-1} respectively when the concentration of the dye increases from 400 to 600 mg.L^{-1}.

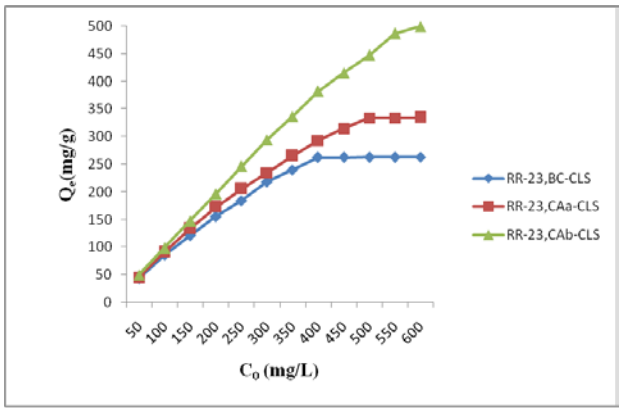

Figure .10. Effect of initial dye concentration on RR-23 adsorption by BC-CLS, CAa-CLS and CAb-CLS (t=60min, T = 30 ± 1 ° C, Adsorbent dose 50mg, stirring = 200 rpm and pH = 10 ± 0.3)

In fact, the increase in concentration induces the elevation of the driving force of the concentration gradient; hence the increase in diffusion of the dye molecules in solution across the surface of the adsorbent which involves the adsorbed amount remains constant.

3.5. The effect of contact time

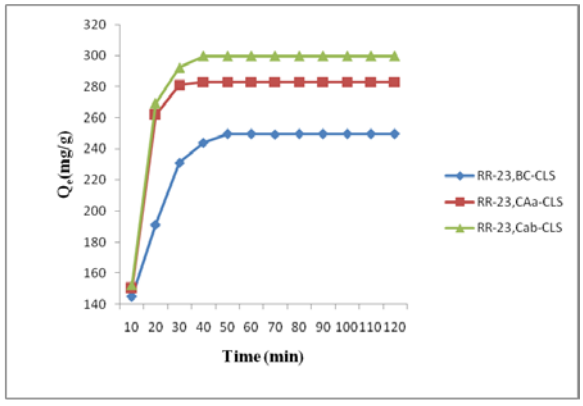

Figure .11. Effect of contact time on dye adsorption by BC-CLS, CAa-CLS and CAb-CLS (T = 30 ± 1 °C, Adsorbent dose 50 mg, C_o=300mg.L^{-1}, stirring = 200 rpm and pH = 10 ± 0.3)

The figure 11 showing the evolution of the adsorbed quantity of the RR-23 dye per gram of BC-CLS, CAa-CLS and CAb-CLS as a function of the contact time at an initial concentration of the dye is 300 mg.L^{-1}, Figure 10 shows that the amount of adsorbate attached to BC-CLS, CAa-CLS and CAb-LSC increase with increasing time from 10 to 40 min with adsorbed amount ranging from 144.88 to 244.09 mg.g^{-1}, from 150.43 to 282.98 mg.g^{-1} and from 152.35 to 299.66 mg.g^{-1} respectively. Thus the adsorption is done with a high speed in the first interval [10.40 min. At times greater than 40 min the adsorbed quantity remains almost constant with a low rate of variation almost equal to 0.15 mg.g^{-1}.

3.6. Kinetics of Adsorption

The best established model for studying adsorption kinetics is selected based on the correlation factor. From the results of figure 12 and table 2, we find that the model with the highest correlation factor is the pseudo-second-order model (R^2 = 0.997, R^2 = 0.996, and R^2=0.995), can infer that the pseudo-second-order model is the one that describes the RR-23 dye adsorption process on the BC-CLS, CAa-CLS and CAb-CLS respectively, we also see that the calculated adsorbed quantities Q_e, cal by this model are closer to experimentally adsorbed quantities $Q_{e,exp}$.

TABLE 2. ADSORPTION KINETICS CONSTANTS OF RR-23 ON BC-CLS, CAA-CLS AND CAB-CLS (T = 30 ± 1 °C, ADSORBENT DOSE 50 MG, C_o=300 MG.L^{-1}, STIRRING = 200 RPM AND PH = 10 ± 0.3)

Model		BC-CLS	CAa-CLS	CAb-CLS
Pseudo -1st Order	**R^2**	**0.900**	**0.885**	**0.889**
	K_1 (*ml.min^{-1}*)	0.119	0.109	0.11
	Q_e (*mg.g^{-1}*)	382.98	80.399	142.31
Pseudo-2nd Order	**R^2**	**0.997**	**0.996**	**0.995**
	K_2 (*g.mg^{-1}.min^{-1}*)	0.0005	0.0007	0.0007
	Q_e (*mg.g^{-1}*)	333.33	333.33	333.33
Elovich	**R^2**	**0.643**	**0.425**	**0.462**
	α (*mg.g^{-1}.min^{-1}*)	310.03	799.39	488.09
	β (*g.mg^{-1}*)	0.026	0.026	0.022
Intraparticular diffusion	**R^2**	**0.796**	**0.585**	**0.625**
	K_i (*mg.g^{-1} min $^{0.5}$*)	10.65	10.08	11.69
	C (*mg.g^{-1}*)	151.9	192.3	194.1

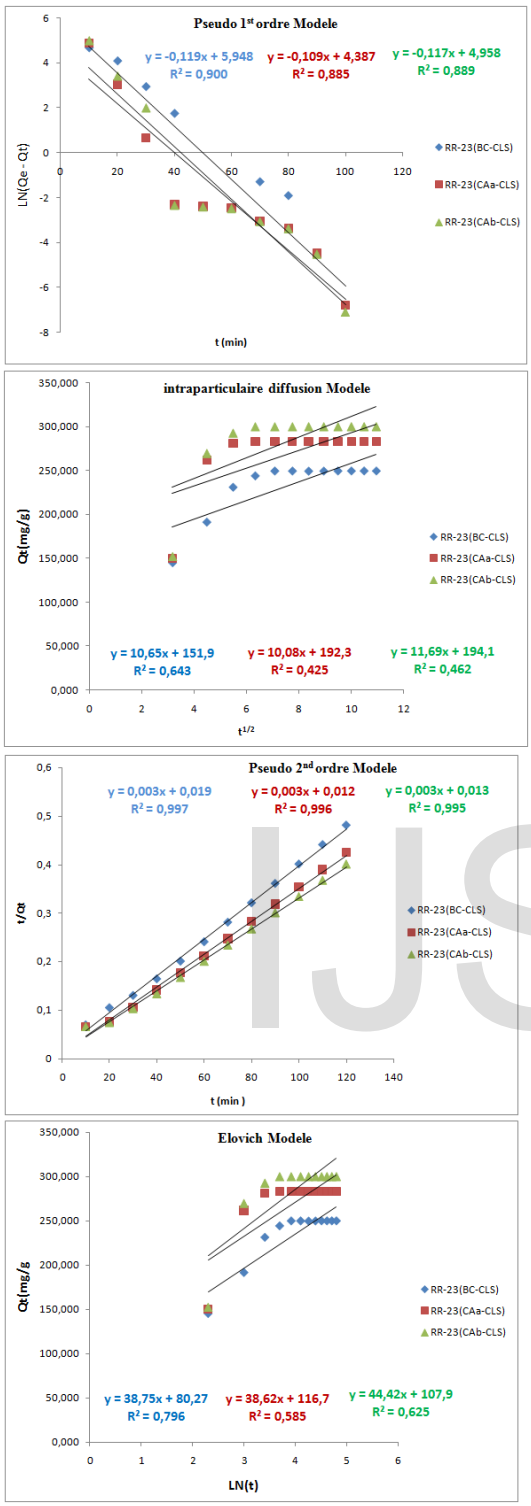

Figure. 12. The four kinetic model of dye adsorption on BC-CLS, CAa-CLS and CAb-CLS (T = 30 ± 1 °C, Adsorbent dose 50 mg, C_o=300 mg.L-1, stirring = 200 rpm and pH = 10 ± 0.3)

3.7. Adsorption isotherms

In this study, the studied models are the model of Langmuir, model of Freundlich, Tempkin and the model dubinin Radushkevich. The most frequently established model for the study of adsorption isotherms is the Langmuir model in Figure 13- (a), 13- (b) and 13- (c). The results obtained are shown in Table 3.

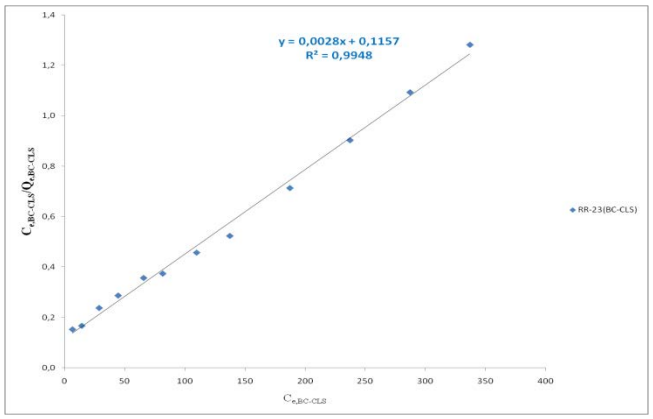

Figure. 13-(a). The Langmuir Isotherms for the adsorption of RR-23 on the BC-CLS (t= 60 min; T=30±1°C, Adsorbent dose 50 mg, stirring = 200 rpm and pH =10± 0.3)

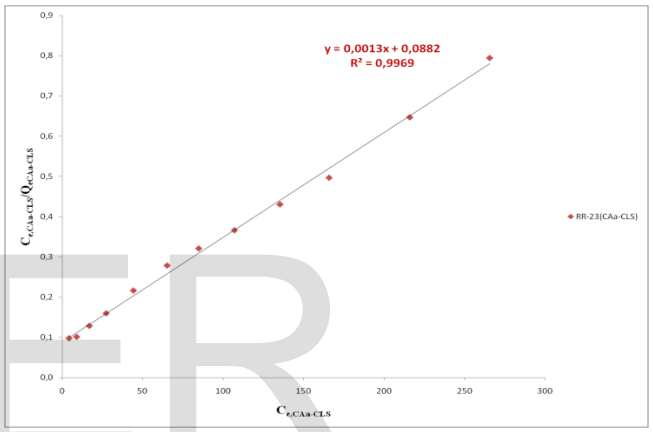

Figure .13 – (b). The Langmuir Isotherms for the adsorption of RR-23 on the CAa-CLS (t= 60 min; T=30±1°C, Adsorbent dose 50 mg; stirring = 200 rpm and pH =10± 0.3))

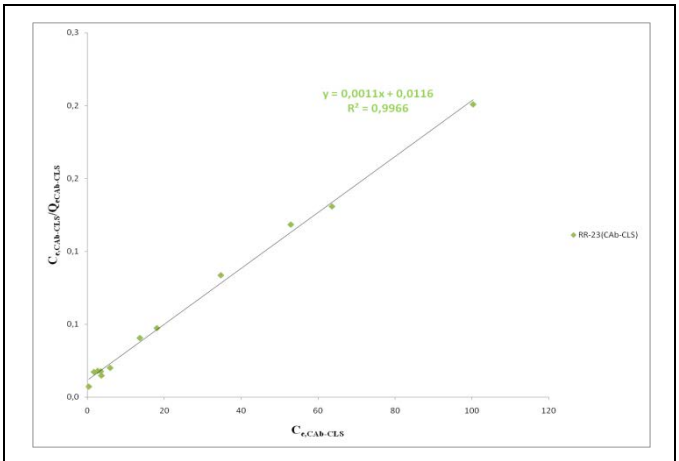

Figure. 13 – (c). The Langmuir Isotherms for the adsorption of RR-23 on the CAb-CLS (t= 60 min; T=30±1°C, Adsorbent dose 50 mg; stirring = 200 rpm and pH =10± 0.3)

TABLE 3. CONSTANT ADSORPTION ISOTHERMS OF RR-23 ON BC-CLS, CAA-CLS AND CAB-CLS (T= 60 MIN; T=30±1°C, ADSORBENT DOSE 50 MG, STIRRING = 200 RPM AND PH =10± 0.3)

Models	Constants	BC-CLS	CAa- CLS	CAb- CLS
Langmuir	**R^2**	**0.9948**	**0.9969**	**0.9966**
	R_L	0.0644-0.04524	0.1018-0.5763	0.0173-0.1742
	K_L *(L.mg^{-1})*	0.0242	0.0147	0.0948
	Q_m *(mg.g^{-1})*	357.143	769.231	909.10
Freundlich	**R^2**	**0.9132**	**0.9422**	**0.8983**
	K_F	25.559	31.218	103.544
	n	2.257	2.150	2.513
Tempkin	**R^2**	**0.9565**	**0.9882**	**0.9654**
	K_T *(L.g^{-1})*	3.271	2.772	3.276
	B_1 *(J.mol^{-1})*	62.380	77.240	88.230
	b	40.364	32.598	28.538
Dubinin-Radushkevich	**R^2**	**0.7693**	**0.7626**	**0.6227**
	K_{ad} *(mol^2.Kj^{-2})*10^{-5}*	0.142	0.074	0.001
	E*(Kj.mol^{-1})*	18.76	25.99	22.36
	Q_m *(mg.g^{-1})*	213.151	265.336	307.969

3.8. Comparison of adsorption capacity with various adsorbents

Table 4 shows the adsorption capacity of dyes and heavy metals in aqueous solutions by activated carbons of different biomass.

TABLE .4 . COMPARISON OF ADSORPTION CAPACITIES OF VARIOUS ADSORBENTS FOR THE REMOVAL OF DYES AND HEAVY METALS ON CHARCOAL ACTIVATED.

Adsorbents	Adsorbent Pollutants	Dose (mg)	C_0 (mg/L)	pH	kinetic	isotherm	Q_m (mg/g)	Ref.
Zinc oxid loeded activated char (ZnO-AC)	OG Rh-b	8 à 30	50	7	Pseudo-second order	Langmuir	153.8 128.2	[21]
Actif charcoal (AC) **Rice straw biochar (RS)** **Wood chip biochar (WC)**	CV-CR	01	500	7	Pseudo-second order	Langmuir	271.0 620.3 195.6	[22]
Charcoal (tree branches) **(BCA-TiO_2)**	MB Cd^{2+}	** **	0.4 600	7 8	Pseudo-second order	***	200 250	[7]
Sulfonated peanut shell (PNS-SO_3H)	MB TC	20	900 ppm	10	Pseudo-second order	Langmuir	1250 303	[23], [24]
Shrimp shell (SS) **Coal acid mine drainage (AMD)**	Mn Fe	**	≤ 1 ≤ 15	6-9 5-9	Pseudo-second order	Freundlich	17.43 3.87	[25]
Coal fly ash (CFA)	MG R6G	40 30	100 ppm	8	Pseudo-second order	Langmuir	233.3 381.7	[26]
Biomass CLS Biochar (BCCLS)	RR-23	50	50	7	Pseudo-second order	Langmuir	62.5 166.67	[2]
Biomass CLSh Biochar (BCCLSh)	RR-23	50	50	7	Pseudo-second order	Langmuir	90.91 354.82	[3]
Biochar BC CLS Biochar (BCCLSh)	AO-52	50	300	7	Pseudo-second order	Langmuir	333.33 500	[27]
Silica-Chitosan Composite	RR-23 RB19	40	60	7	Pseudo-second order	Langmuir	128.2 156.25	[5]
Chitosan Composite MCs/MS	RR-23 RB19 Fe^{2+}	70	50	7	Pseudo-second order	Langmuir Freundlich Freundlich	71.94 175.44 62.11	[4]
Activated Carbon Derived From Phragmites Australis	MO MV	50 50	500 400	**	Pseudo-second order	Langmuir	238.11 476.19	[28]
Carbon nanotubes (CNTs)	MO	200mg/L	10	**	Pseudo-second order	Langmuir	55.2	[29]
Charbon of Quercus Brantii (Oak)	ACT IBP	1g/L	100	7	Pseudo-second order	Freundlich	45.45 96.15	[30]
BC-CLS	**RR-23**	**50**	**300**	**10**	**Pseudo-second order**	**Langmuir**	**357.143**	**This Work**
CAa-CLS	**RR-23**	**50**	**300**	**10**			**769.23**	
CAb-CLS	**RR-23**	**50**	**300**	**10**			**909.1**	

The Table 4 shows, the majority of the activated carbons used in the removal of the anionic dyes, cationic dyes and heavy metals have adsorbed quantities of less than 500 $mg.g^{-1}$, except that Rice straw charcoal has an adsorbed quantity equal to 620.3 $mg.g^{-1}$, that the Sulfonated peanut shell that presents the maximum order quantity 1250$mg.g^{-1}$. But we result for the elimination of the most used textile dyes and the most existing in the effluent as RR-23 in industrial waters by the activated charcoal of the cistusLadaniferus seeds presents a very important adsorbed quantity 769.23$mg.g^{-1}$ for the CAa-CLS and 909.1$mg.g^{-1}$ for CAb-CLS.

4. CONCLUSION

The valorization of activated charcoal obtained by fixed bed pyrolysis from cistus Ladaniferus seeds as bioadsorbents of anionic dyes in water treatment and especially for the discoloration of effluents used in the textile industry (elimination of anionic dyes RR-23). The raw materials we used as adsorbents are 03, which are derived from forest waste. These are BC-CLS, CAa-CLS, and CAb-CLS. These materials have been characterized by DRX, IRTF, MEB, and EDXA. Next, we studied several parameters such as pH effect, adsorbent dose, contact time and initial concentration. The adsorption kinetics of these three materials described by the pseudo-second-order model and the adsorption isotherms follow the Langmuir isotherm. The adsorption capacity of the RR-23 dye is equal to 357.143 $mg.g^{-1}$ for BC-CLS, 769.231 $mg.g^{-1}$ for CAa-CLS and 909.1 $mg.g^{-1}$ for CAb-CLS. The elimination yield reached 86.77% for BC-CLS shell biochar and 91.11% for CAa-CLS and 99.29% for CAb-CLS.

Acknowledgment

This work is the result of a research on the valorization of the bioresource in the laboratory of engineering chemistry and valorization of resources of faculty of sciences and technical in Tanger- Morocco.

References:

[1] H. El Farissi, R. Lakhmiri, H. El Fargani, A. Albourine, M. Safi, "Valorisation of a Forest Waste (Cistus Seeds) for the Production of Bio-Oils," *Journal of materials and Environmental Sciences*, vol. 8, no. 2, pp. 628–635, 2017.

[2] H. El Farissi, R. Lakhmiri, A. Albourine, M. Safi, O. Cherkaoui, "Removal of RR-23 dye from industrial textile wastewater by adsorption on cistus ladaniferus seeds and their biochar," *Journal of Environment and Earth Science*, vol. 7, no. 11, pp. 105–118, 2017.

[3] H. El Farissi, R. Lakhmiri, A. Albourine, M. Safi, and O. Cherkaoui, "Removal of anionic dyes from aqueous solutions by cistus ladaniferus shells and their biochar: Isotherms, kinetic and thermodynamic studies," *International Journal of Scientific & Engineering Research*, vol. 9, no. 11, pp. 200–211, 2018.

[4] H. El Fargani, R. Lakhmiri, H. El Farissi, A. Albourine, M. Safi and O. Cherkaoui, "Modified Chitosan Immobilized on Modified Sand for Industrial Wastewater Treatment in Multicomponent Sorption : Shrimp Biowaste Processing,"*Chemistry and Materials Research*, vol. 9, no. 4, pp. 20–42, 2017.

[5] H. El Fargani, R. Lakhmiri, H. El Farissi, A. Albourine, M. Safi, and O. Cherkaoui, "Removal of anionic dyes by silica-chitosan composite in single and binary systems : Valorization of shrimp co- product ' Crangon - Crangon ' and ' Pandalus Borealis ,'" *Journal of Materials and Environmental Sciences*, vol. 8, no. 2, pp. 724–739, 2017.

[6] S. S. Wei wang, Yan-Yan Liw, Xian-feng Chen, "Facile Synthesis Fishbone Charcoal (FBC) with Remarkable Adsorption towards Methylene Blue," *Procedia Engineering*, vol. 211, pp. 495–505, 2018.

[7] N. Popa and M. Visa, "The synthesis, activation and characterization of charcoal powder for the removal of methylene blue and cadmium from wastewater," *Advanced Powder Technology*, vol. 28, no. 8, pp. 1866–1876, 2017.

[8] R. Baccar, M. Sarrà, J. Bouzid, M. Feki, and P. Blánquez, "Removal of pharmaceutical compounds by activated carbon prepared from agricultural by-product," *Chemical Engineering Journal*, vol. 211–212, no. 2012, pp. 310–317, 2012.

[9] Q. L. Y. Sun, Q. Yue, B. Gao, L. Huang. X. Xu, "Comparative study on characterization and adsorption properties of activated carbons with H3PO4 and H4P2O7 activation employing Cyperus alternifolius as precursor," *Chem. Eng. J*, vol. 181–182, pp. 790–797, 2012.

[10] T.-H. Liou., "Development of mesoporous structure and high adsorption capacity of biomass-based activated carbon by phosphoric acid and zinc chloride activation," *Chem. Eng. J*, vol. 158, pp. 129–142, 2010.

[11] V. L. Cazetta, A. M.M. Vargas, E. M. Nogami, M. H. Kunita M. R. Guilherme, A. C. Martins, T. L. Silva, J. C. G. Moraes, "NaOH-activated carbon of high surface area produced from coconut shell: kinetics and equilibrium studies from the methylene blue adsorption," *Chem. Eng. J.*, vol. 174, pp. 117–125, 2011.

[12] N. Nasuha, B. H. Hameed., "Adsorption of methylen blue from aqueous solution onto NaOH -modified rejected tea," *Chem. Eng. J.*, vol. 166, pp. 783–786, 2011.

[13] S. Lagergren, Hand.,vol. 24, pp. 1–39, 1898.

[14] Y.-S. HO, "Citation review of Lagergren kinetic rate equation on adsorption reactions," vol. 59, no. 1, pp. 171–177, 2004.

[15] Y.S. Ho and G. McKay, "Pseudo - second order model for sorption processes", *Process Biochemistry* vol. 34, pp. 451 – 465, 1999.

[16] Y.S. Ho, G. McKay, *Chem. Eng. J.* vol. 70, pp. 115–124, 1998.

[17] S.H. Chien and W.R. Clayton, "Application of Elovich equation to the kinetics of phosphate release and sorption in soils.," *SoilSci. Soc. Am. J.*, vol. 44, pp. 265–268, 1980.

[18] K.Urano and T. Hirotaka, 'Process Development for Removal and Recovery of Phosphorus from Wastewater by a New Adsorbent. 2. Adsorption Rates and Breakthrough Curves' Ind. *Eng. Chem. Res. vol.* 30, pp. 1897-189, 1991.

[19] M. Ghasemi, H. Javadian, N. Ghasemi, S. Agarwal, and V.K. Gupta, *Journal of Molecular Liquids*, vol. 215, pp. 161–169, 2016.

[20] K. Sujoy, Das, R. Jayati, R. Akhil, and A. K. Guha, "Adsorption Behavior of Rhodamine B on Rhizopus o ryzae Biomass," *Langmuir*, vol. 22, no. 17, pp. 7265–7272, 2006.

[21] J. Saini, V. K. Garg, R. K. Gupta, and N. Kataria, "Removal of Orange G and Rhodamine B dyes from aqueous system using hydrothermally synthesized zinc oxide loaded activated carbon (ZnO-AC)," *Journal of Environmental Chemical Engineering*, vol. 5, no. 1, pp. 884–892, Feb. 2017.

[22] D. D. Sewu, P. Boakye, and S. H. Woo, "Highly efficient adsorption of cationic dye by biochar produced with Korean cabbage waste," *Bioresource Technology*, vol. 224, pp. 206–213, 2017.

[23] M. T. Islama, AHM. Golam Hyderb, R. Saenz-Aranaa, C. Hernandeza, T. Guintoa, A. Ahsana, B. Alvarado-Tenorioc, J. Noverona, "Removal of methylene blue and tetracycline from water using peanut shell derived adsorbent prepared by sulfuric acid reflux," *Journal of Environmental Chemical Engineering*, vol. 7, no. 1, pp. 1-12, 2019.

[24] K. M. Isa, S. Daud, N. Hamidin, K. Ismail, S. A. Saad, and F. H. Kasim, "Thermogravimetric analysis and the optimisation of bio-oil yield from fixed-bed pyrolysis of rice husk using response surface methodology (RSM)," *Industrial Crops and Products*, vol. 33, no. 2, pp. 481–487, 2011.

[25] D. Núñez-gómez, C. Rodrigues, and F. Rubens, "Adsorption of heavy metals from coal acid mine drainage by shrimp shell waste : Isotherm and continuous-flow studies,"*Journal of Environmental Chemical Engineering*, vol. 7, no. 1, pp. 1–10, 2019.

[26] S. Dash, H. Chaudhuri, R. Gupta, and U. G. Nair, "Adsorption Study of Modified Coal Fly Ash with Sulfonic Acid as a Potential Adsorbent for the Removal of Toxic Reactive Dyes from Aqueous Solution: Kinetics and Thermodynamics," *Biochemical Pharmacology*, no. https://doi.org/10.1016/j.jece.2018.05.017, 2018.

[27] H. El Farissi, R. Lakhmiri, A. Albourine, and M. Safi, "The adsorption of the orange acid dye 52 in aqueous solutions by the biochar of the seeds and shells of Cistus Ladaniferus," *International Journal of Scientific & Engineering Research*, vol. 9, no. 10, pp. 563–571, 2018.

[28] S. Chen, J. Zhang, C. Zhang, Q. Yue, Y. Li, and C. Li, "Equilibrium and kinetic studies of methyl orange and methyl violet adsorption on activated carbon derived from Phragmites australis," *Desalination*, vol. 252, no. 1–3, pp. 149–156, 2010.

[29] D. Zhao, W. Zhang, C. Chen, and X. Wang, "Adsorption of Methyl Orange Dye Onto Multiwalled Carbon Nanotubes," *Procedia Environmental Sciences*, vol. 18, pp. 890–895, 2013.

[30] H. Nourmoradi, K. F. Moghadam, A. Jafari, and B. Kamarehie, "Removal of Acetaminophen and Ibuprofen from Aqueous Solutions by Activated Carbon Derived from Quercus Brantii (Oak) Acorn as a Low-cost Biosorbent," *Biochemical Pharmacology*, no. https://doi.org/10.1016/j.jece.2018.10.047, 2018.